Green Cooperative Spectrum Sensing and Scheduling in Heterogeneous Cognitive Radio Networks

Abdulkadir Celik and Ahmed E. Kamal
Dept. of Electrical and Computer Eng., Iowa State University, Ames, Iowa, 50011

***Abstract*—In this paper we consider heterogeneous cognitive radio networks (CRNs) comprising primary channels (PCs) with heterogeneous characteristics and secondary users (SUs) with various sensing and reporting qualities for different PCs. We first define the opportunity as the achievable total data rate and its cost as the energy consumption caused from *sensing*, *reporting* and *channel switching* operations and formulate a joint spectrum discovery and energy efficiency objective to minimize the energy spent per unit of data rate. Then, a mixed integer non-linear programming problem is formulated to determine: 1) the optimal subset of PCs to be scheduled for sensing, 2) the SU assignment set for each scheduled PC, and 3) sensing durations and detection thresholds of each SU on PCs it is assigned to sense. Thereafter, an equivalent convex framework is developed for specific instances of the above combinatorial problem. For comparison, optimal detection and sensing thresholds are also derived analytically under the homogeneity assumption. Based on these, a prioritized ordering heuristic (POH) is developed to order channels under the spectrum, energy and spectrum-energy limited regimes. After that, a scheduling and assignment heuristic (SAH) is proposed and is shown to perform very close to the exhaustive optimal solution. Finally, the behavior of the CRN is numerically analyzed under these regimes with respect to different numbers of SUs, PCs and sensing qualities.**

***Index Terms*—Energy and throughput efficient, cooperative spectrum sensing, multi-channel sensing scheduling, Poisson-Binomial, channel switching.**

I. Introduction

A. Motivation and Background

The motivation behind the CRNs is rooted in the insufficiency of the current inflexible spectrum allocation policy to meet the ever-increasing demands of today's wireless communication networks. Cognitive radios (CRs) are introduced to detect and utilize unused spectrum bands in an opportunistic manner such that primary users (PUs), who are incumbent licensees, are protected against performance degradation caused by CRs which are also known as secondary users (SUs). Furthermore, a substantial part of this demand has recently migrated to mobile wireless networks and devices with limited energy resources. Considering the fact that 30% of the energy expenditure of mobile devices is caused by wireless networking and computing [1], energy efficient (EE) cognitive radio networks play a vital role to provide portable devices with more spectrum for less energy consumption. Optimizing energy utilization not only leads to a more affordable network with reduced cost, but also an environmentally friendly network [2]. Because approximately 2% of the worldwide CO_2 emissions is caused by the communications and information technologies [3], energy efficient policies are becoming more important to achieve green communication standards.

Nonetheless, modeling an EE-CRN is not trivial since it involves designers in many tradeoffs to be balanced and many real life challenges to be taken care of. In particular, the detector performance of individual SUs is substantially degraded by the channel impairments such as path loss, multipath fading and shadowing etc. To surmount this issue, *cooperative spectrum sensing* (CSS) is addressed to be an effective method which achieves more reliable detection by exploiting the spatio-temporal diversity of SUs. However, cooperation is not free of energy overhead and there are three leading energy consumptive factors in a multi-channel CSS scheduling (CSSS) framework: 1) *channel switching energy*, 2) *sensing energy*, and 3) *reporting energy*. The sum of those can be referred to as the *opportunity cost*. Defining the achievable total data rate as a commodity and the opportunity cost as currency, we will deal with minimization of the currency expenditure per earned commodity under a heterogeneous CRN scenario where PCs have different probabilities of being idle and SUs have different reporting errors and sensing qualities (i.e. signal-to-noise-ratio (SNR)) for different primary channels (PCs).

B. Related Work

Some of recent research efforts can be exemplified as follows: By successively activating a subset of sensors to sense the spectrum and putting others into a sleep mode, an energy efficient CSS with an optimal scheduling method is considered for sensor aided CRNs [4]. Zhang and Tsang prove the energy efficiency optimality of the myopic policy using the framework of partially observable Markov decision process in [5]. Sun et al. consider a heterogeneous CRN scenario and develop a CSSS framework using a discrete-convex formulation in three steps. They use the OR voting rule in their analysis to maximize a utility function as a weighted sum of capacity and energy expenditure [6]. Eryigit and others try to minimize total sensing and reporting energy consumption using OR voting rule in an error-free cooperation environment. They provide efficient heuristic methods after solving the combinatorial problem via outer linearization methods [7]. Even though all these previous studies have important contributions, they lack the generality of exploitation different voting rules and energy efficiency by assuming AND/OR voting rule for the sake of tractability. However, the majority voting rule is already pointed out to be the best voting rule in the context of additional SNR requirement to achieve ideal performance [8] and to be the most energy efficient to achieve the energy efficiency of ideal cooperation scheme [9]. This is recently re-validated

by [10] where the authors use discrete-convexity tools to maximize the achievable throughput in both homogeneous and heterogeneous scenarios. Another shortcoming of the works in [5] - [7], [10] is the assumption of the perfect reporting environment. However, the existence of a reporting error wall is clearly demonstrated in [8]- [9] such that after this error wall no reliable cooperation is possible regardless of how much energy is spent.

Channel switching delay and energy is another practical concern in multi-channel CSSS, which is not considered in above references. In [11] and [12], channel switching factor is taken into account in the realm of resource allocation scheduling. In [13], the authors propose a scheduling method which minimizes the energy cost caused by sensing, reporting and channel switching actions under the assumption that the number of SUs is much more than the number of PUs while employing the OR fusion rule under perfect reporting channel conditions. The authors in [14] propose a framework to minimize the ratio of summary of sensing-reporting-switching cost and the discovered spectrum under erroneous reporting and generalized voting rules.

C. Main Contributions

Our main contributions can be summarized as follows:

1) We couple the energy and spectrum efficiency as a single objective such that the energy spent per achieved data rate is minimized subject to global detection and false alarm constraints to protect PUs from SU interference and ensure a certain spectrum utilization, respectively. Assuming SUs have different sensing and reporting characteristics, a mixed integer non-linear programming (MINLP) problem is formulated to determine: a) the optimal subset of PCs to be scheduled for sensing, b) the SU assignment set for each scheduled PC, and c) sensing durations and detection thresholds of each SU on PCs it is assigned to sense. Assuming that switching time satisfies the linearity and triangularity properties [11] - [12], we also formulate the optimal sensing order to minimize the channel switching latency and energy as a linear function of the total frequency distance .
2) A heterogeneous K-out of-N rule is first proposed in order to allow SUs to have different detection accuracy according to their sensing and reporting qualities. For given specific instances of the above combinatorial problem and real valued number of samples, an equivalent convex framework is then developed for the proposed K-out of-N rule. As a comparison, we derive the closed form expressions for optimal detection and sensing thresholds of the traditional homogeneous K-out of-N rule which equivalently treats each SU regardless of their sensing and reporting features by enforcing them to have identical local detector performances.
3) Exploiting the proposed convex framework, prioritized ordering heuristic (POH) is developed in order to order channels under spectrum, energy and spectrum-energy limited regimes. Based on POH, a scheduling and assignment heuristic (SAH) is proposed and shown to have a very close performance to the exhaustive solution. The behavior of the CRN is then studied under these regimes with respect to different numbers of SUs, PCs and SNR distributions.

D. Paper Organization

The rest of this paper is organized as follows: Section-II introduces the system model. After that, section III provides the details of CSS under heterogeneity and homogeneity modes. Section IV derives the coupled energy and spectrum efficiency, and then formulates the problem. Section V develops the POH and SAH algorithms. Finally, simulation results and analysis are presented in Section VI and Section VII concludes the paper with a few remarks.

II. System Model

We consider a large scale CRN scenario where the sensing scheduling of PCs and the assignment of SUs to sense scheduled PCs are determined by a central cognitive base station (CBS). The numbers of PCs and SUs are denoted by M and N, respectively. Similarly, the set of scheduled PCs and the set of assigned SUs are denoted as $\mathcal{M}$ and $\mathcal{N}$, respectively. The subset of $\mathcal{N}$ assigned to sense the same PC is referred to as a *cluster* and SUs can join more than one cluster at a time. We assume that the CBS has the information about the sensing and reporting qualities of SUs and chooses a cluster head (CH), which undertakes the role of fusion center, for each cluster. After the determination of CHs, report and control signaling between the SUs and CBS are exchanged over an erroneous common control channel (CCC) via the CHs. We assume that SUs operate in a time-slotted fashion and experience flat fading such that PC states do not change within a time slot duration, which is necessary in practice for tractability of the performance analysis. Time-slotted operation of the secondary network is depicted in Fig. 1 where each timeslot of duration T is split into two stages: 1) *channel search* to discover spectrum holes and 2) *channel utilization* for secondary data transmission.

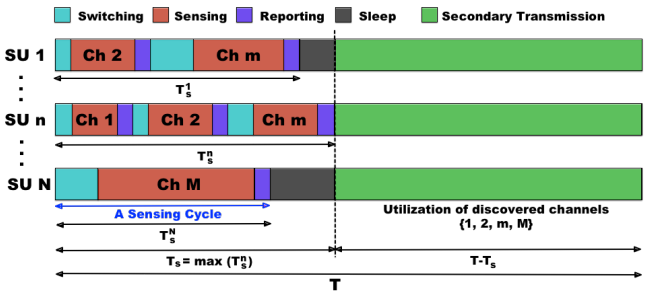

Fig. 1: Demonstration of a scheduling timeslot consisting of switching-sensing-reporting cycles and secondary data transmission.

In the former, channel searching proceeds in switching-sensing-reporting *cycles* where an SU n first performs *channel switching* to adjust its operating frequency to the assigned PC m, then executes *sensing* for a required duration, and finally reports its local decision to the CH in order to receive

a global decision feedback regarding the PC state. After collecting and fusing all local hard decisions, the CH reports its global hard decision about the channel occupancy state to the CBS. Accordingly, the channel search time of SU n, T_s^n, is determined by the summation of sensing cycles of all assigned PCs. We note that the duration of the channel search stage, thus the residual time for the channel utilization, is determined by the slowest SU since the CBS needs to wait for the arrival of all decisions to make the global decisions and resource allocation policy which is beyond the scope of this paper. Therefore, channel search duration is given by

$$T_s = \max_{n \in \mathcal{N}} (T_s^n) \tag{1}$$

In the latter part of the slot, discovered free channels are utilized by SUs in the remaining available time, $T - T_s$, according to a certain resource sharing strategy. In case an SU completes all necessary cycles before T_s, it puts itself into a sleep mode to save energy until it is allowed to utilize the discovered channels. Furthermore, if an SU has undesirable sensing and reporting characteristics which degrades the overall secondary network performance, optimal scheduling policy may put it into sleep mode to save energy. Intuitively, there exists a fundamental tradeoff between channel search and channel utilization duration such that while sensing more channels for longer durations results in the discovery of more bandwidth with higher accuracy, this degrades the throughput of the secondary network as it reduces the time left for channel utilization. This fundamental tradeoff is also a way of limiting the energy cost of SUs since the channel search duration is jointly minimized to decrease and increase the opportunity and its cost, respectively. For the remainder of the paper, we define the following matrices and vectors to formulate the scheduling problem in a more compact way:

- $\boldsymbol{y} \in \{0,1\}^M$ is a vector of binary variables y_m which indicates that the PC m is scheduled to be sensed or not.
- $\boldsymbol{X} \in \{0,1\}^{M \times N}$ is a binary PU↔SU assignment matrix with entries $x_m^n \in \{0,1\}$ which indicates that SU n is committed to sense PC m if it is non-zero.
- $\boldsymbol{S} \in \mathbb{N}^{+^{M \times N}}$ is a positive real matrix with entries S_m^n which defines the number of samples of SU n on PC m.
- $\boldsymbol{\mathcal{E}} \in \mathbb{R}^{M \times N}$ is a real matrix with entries ε_m^n which defines the detection threshold of the SU n on PC m.
- $\boldsymbol{\Gamma} \in \mathbb{R}^{+^{M \times N}}$ is a positive real matrix with entries γ_m^n which represents the SNR of SU n on PC m.
- $\boldsymbol{P} \in \mathbb{R}^{M \times N}$ is the reporting bit error rate matrix with entries $p_m^n \in [0,1]$ which represents the reporting error between SU n and the CH.
- $\boldsymbol{f} \in \mathbb{R}^{+^M}$ is a vector with entries f_m^c which represents the carrier frequency of the PC m.

III. Cooperative Spectrum Sensing (CSS)

A. Heterogeneous Mode

Since the focus of this paper is the scheduling aspects of the CSS, a generic sensing method like *energy detection* is adequate for this purpose. Energy detectors (EDs) have been extensively exploited as the ubiquitous sensing technique in the literature due to its simplicity, compatibility with any signal type, and low computational and implementation complexity [15]. To detect primary signals, ED of SU $n \in \mathcal{N}$ measures the received signal energy on PC $m \in \mathcal{M}$ for a number of samples S_m^n and compares it with a detection threshold ε_m^n to make a local decision on binary hypotheses $\mathcal{H}_m^0$ and $\mathcal{H}_m^1$ which represent the absence and presence of PUs, respectively. For a large S_m^n and normalized noise variance, the probability of false alarm, $P_{m,n}^f = \mathcal{P}[\mathcal{H}_1|\mathcal{H}_0]$, and the probability of detection, $P_{m,n}^d = \mathcal{P}[\mathcal{H}_1|\mathcal{H}_1]$, are respectively given by [16]

$$P_{m,n}^f\left(S_m^n, \varepsilon_m^n\right) = \mathcal{Q}\left[\left(\varepsilon_m^n - 1\right)\sqrt{S_m^n}\ \right] \tag{2}$$

$$P_{m,n}^d\left(S_m^n, \varepsilon_m^n, \gamma_m^n\right) = \mathcal{Q}\left[\left(\varepsilon_m^n - \gamma_m^n - 1\right)\sqrt{\frac{S_m^n}{2\gamma_m^n + 1}}\ \right] \tag{3}$$

where $\gamma_m^n \neq \gamma_{m'}^{n'}, \forall m \neq m', \forall n \neq n'$ is the SNR of SU n on the PC m, which is obtained by the combined path loss and shadowing model [17], and $\mathcal{Q}(x) = \frac{1}{\sqrt{2\pi}} \int_x^{+\infty} e^{-y^2/2} dy$ denote the right-tail probability of a normalized Gaussian distribution, respectively.

After the local sensing process, SU n sends its hard result u_m^n to the CH over a binary symmetric CCC. Defining the error probability as $p_m^n = \mathcal{P}\left[\tilde{u}_m^n = 1 | u_m^n = 0\right] = \mathcal{P}\left[\tilde{u}_m^n = 0 | u_m^n = 1\right]$ where $\tilde{u}_m^n$ is the hard decision received by the CH, the local false alarm and detection probabilities received at the CH side are given by

$$\tilde{P}_{m,n}^f\left(P_{m,n}^f\right) = p_m^n\left(1 - P_{m,n}^f\right) + \left(1 - p_m^n\right) P_{m,n}^f \tag{4}$$

$$\tilde{P}_{m,n}^d\left(P_{m,n}^d\right) = p_m^n\left(1 - P_{m,n}^d\right) + \left(1 - p_m^n\right) P_{m,n}^d \tag{5}$$

Denoting the cluster set for PC m as $\mathcal{C}_m$ with the cardinality $C_m = \sum_{n \in \mathcal{N}} x_m^n$, the CH collects $\tilde{u}_m^n$'s and make the global decision using the following test

$$\mathcal{K}_m = \sum_{n \in \mathcal{C}_m} \tilde{u}_m^n x_m^n \underset{\mathcal{H}_m^0}{\overset{\mathcal{H}_m^1}{\gtrless}} \kappa_m \tag{6}$$

which follows the *Poisson-Binomial* distribution with the following conditional probability density functions [18]

$$p\left(\kappa_m | \mathcal{H}_0\right) = \sum_{A \in F_{\kappa_m}} \prod_{j \in A} \tilde{\boldsymbol{P}}_{\boldsymbol{m}}^{\boldsymbol{f}}(j) \prod_{j \in A^c} \left(1 - \tilde{\boldsymbol{P}}_{\boldsymbol{m}}^{\boldsymbol{f}}(j)\right) \tag{7}$$

$$p\left(\kappa_m | \mathcal{H}_1\right) = \sum_{A \in F_{\kappa_m}} \prod_{j \in A} \tilde{\boldsymbol{P}}_{\boldsymbol{m}}^{\boldsymbol{d}}(j) \prod_{j \in A^c} \left(1 - \tilde{\boldsymbol{P}}_{\boldsymbol{m}}^{\boldsymbol{d}}(j)\right) \tag{8}$$

where $\tilde{\boldsymbol{P}}_{\boldsymbol{m}}^{\boldsymbol{f}} = \{\tilde{P}_{m,n}^f | x_m^n = 1, \forall n\}$, $\tilde{\boldsymbol{P}}_{\boldsymbol{m}}^{\boldsymbol{f}}(j) = \tilde{P}_{m,j}^f$, $\tilde{\boldsymbol{P}}_{\boldsymbol{m}}^{\boldsymbol{d}} = \{\tilde{P}_{m,n}^d | x_m^n = 1, \forall n\}$, $\tilde{\boldsymbol{P}}_{\boldsymbol{m}}^{\boldsymbol{d}}(j) = \tilde{P}_{m,j}^d$, and F_{κ_m} is the set of all subsets of κ_m integers that can be selected from $\mathcal{C}_m$. Substituting (4) and (5) in (7) and (8), respectively, the global false alarm and detection probabilities are given in the form of the conditional cumulative distribution function as

$$\begin{aligned} Q_m^f(\tilde{\boldsymbol{P}}_{\boldsymbol{m}}^{\boldsymbol{f}}) &= 1 - \mathcal{P}\left[\mathcal{K}_m \leq \kappa_m - 1 | \mathcal{H}_m^0\right] \\ &= \sum_{i=\kappa_m}^{C_m} p\left(i | \mathcal{H}_m^0\right) \end{aligned} \tag{9}$$

$$\begin{aligned} Q_m^d(\tilde{\boldsymbol{P}}_{\boldsymbol{m}}^{\boldsymbol{d}}) &= 1 - \mathcal{P}\left[\mathcal{K}_m \leq \kappa_m - 1 | \mathcal{H}_m^1\right] \\ &= \sum_{i=\kappa_m}^{C_m} p\left(i | \mathcal{H}_m^1\right) \end{aligned} \tag{10}$$

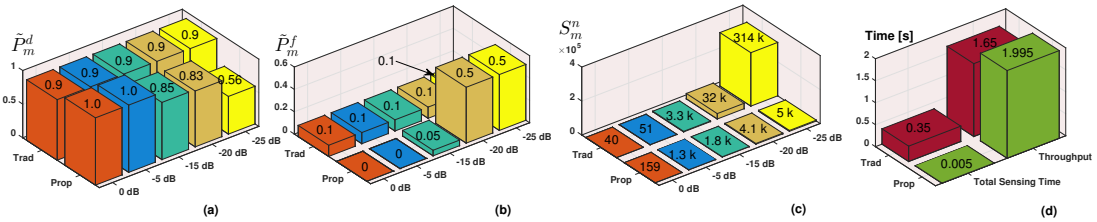

Fig. 2: Comparison of heterogeneous (proposed) and homogeneous (traditional) modes.

which can expeditiously be calculated from polynomial coefficients of the probability generating function of $\mathcal{K}_m$ in order of $\mathcal{O}\left(C_m \log_2 C_m\right)$ [19].

B. Homogeneous Mode

As a special and traditional case, homogeneous mode imposes the condition that SUs must satisfy $\tilde{P}^f_{m,n} = \tilde{P}^f_m,\ \tilde{P}^d_{m,n} = \tilde{P}^d_m,\ \forall n$ regardless of their non-identical SNRs and reporting errors. This yields the well-known K-out of-N rule with Binomially distributed $\mathcal{K}_m$ which is not always energy and throughput efficient. In order to compare proposed heterogeneous CSS scheme with the traditional homogeneous CSS in existing studies, we consider an example heterogeneous cluster consisting of 5 SUs with SNRs $[0, -5, -15, -20, -25]$ dB. Since we are interested in a comparison of sensing cost of the traditional and proposed approaches, we assume $p^n_m = 10^{-3}, \forall m$. Using majority voting rule ($\kappa_m = 3$) and global false alarm (detection) probability targets of $Q^f_{th} = 0.01$ ($Q^d_{th} = 0.99$), Fig. 2 demonstrates the results for homogeneous and heterogeneous modes. In Fig. 2.a-b, while traditional approach enforces SUs to report with identical local detection and false alarm probabilities of 0.9 and 0.1, respectively, proposed method enforces SUs with relatively high SNRs to have near perfect detection and false alarm probabilities. For the values in Fig. 2.a-b, Fig. 2.c demonstrates the sensing duration in terms of the number of samples where it clearly reveals the fact that traditional approach especially requires large S^n_m for the slowest SU with the lowest SNR. However, proposed method alleviate the negative effect of the slowest SU by relaxing its local detector performance. Accordingly, Fig. 2.d demonstrates superiority of the proposed method in terms of the total sensing duration (thus sensing energy) and available room for secondary data transmission after the sensing period within a time frame.

IV. CSS Scheduling Optimization

The ultimate design goal of an energy and spectrum efficient CSS scheduling scheme would be minimizing the energy expenditure per transmitted bit, i.e, [Joules/bit]. On the one hand, such a purpose requires minimization of the opportunity cost via joint optimization of SU assignment along with the determination of sensing durations and detection thresholds with the consideration of distinctive sensing and reporting qualities of SUs subject to collision constraint regulations. On the other hand, it necessitates the maximization of the achievable total throughput by scheduling optimal set of PCs and maximization of the available time left for SU transmission, $T - T_s$.

A. Energy and Spectrum Efficiency

Energy and spectrum efficiency of the CSS scheduling problem can be coupled into a single objective by minimizing the energy cost per obtained opportunity which can be formulated as the number of bits transmitted on discovered free PCs. The opportunity cost is primarily induced from three factors: *channel switching cost*, *sensing cost*, and *reporting cost*.

1) Channel Switching Energy: To execute sensing assignments, SUs have to switch its operating frequency to desired channel's parameters in the beginning of corresponding cycles. We assume that the switching time satisfies the triangularity and linearity properties, i.e., $\tau_{sw} = \beta \times |f^c_{m-1} - f^c_m|$ where β is a switching factor that depends on parameters such as power consumption and used technology [11]- [12]. Based on the initial channel state, ordering the assigned PCs and starting to sense from the closest channel is the optimal policy as it is the shortest path. To formulate the optimal total switching time of the SU n, T^n_{sw}, we define the following vectors: the initial channel state of SU n, $\boldsymbol{x^0_n} \in \{0,1\}^M$ with zero entries except at the intitial frequency, the n^{th} column vector of $\boldsymbol{X}$, $\boldsymbol{x_n}$, $\boldsymbol{f_n} = \boldsymbol{x_n} \circ \boldsymbol{f}$, and $\boldsymbol{f^0_n} = \boldsymbol{x^0_n} \circ \boldsymbol{f}$ where $(\circ)$ denotes the Schur product. Based on optimal T^n_{sw} formulated in (12), the total switching energy expenditure is given by

$$E_{SW}(\boldsymbol{X}) = P_{sw} T_{sw} = P_{sw} \sum_{n \in \mathcal{N}} T^n_{sw}\left(\boldsymbol{x}_n\right) \qquad (11)$$

where P_{sw} and T_{sw} denote the channel switching power and total channel switching time, respectively.

2) Sensing Energy: Denoting the time spent per sample as τ_s, the total energy expenditure for sensing is given by

$$E_S(\boldsymbol{X}, \boldsymbol{S}) = P_s T_{sns} = P_s \tau_s \boldsymbol{e_s}^T \left(\boldsymbol{S} \circ \boldsymbol{X}\right) \tilde{\boldsymbol{e}}_{\boldsymbol{s}} \qquad (13)$$

where P_s is the sensing power and T_{sns} is the total sensing duration of SUs. In (13), $\boldsymbol{e_s}$ and $\tilde{\boldsymbol{e}}_{\boldsymbol{s}}$ are unit vectors with sizes M and N, respectively.

3) Reporting/Controlling Energy: Similarly, denoting the time spent for reporting as τ_r and assuming it is the same for all SUs, the total energy expenditure for reporting is given by

$$E_R(\boldsymbol{X}) = P_r T_r = P_r \tau_r \ \boldsymbol{e_s}^T \boldsymbol{X} \tilde{\boldsymbol{e}}_{\boldsymbol{s}} \qquad (14)$$

where P_r is the sensing power and T_r is the total reporting/controlling duration of SUs. Hence, the opportunity cost can be expressed as

$$E(\boldsymbol{X}, \boldsymbol{S}) = E_{SW}(\boldsymbol{X}) + E_S(\boldsymbol{X}, \boldsymbol{S}) + E_R(\boldsymbol{X}) \qquad (15)$$

$$T_{sw}^{n}\left(\boldsymbol{x}_n\right)=\beta\times\left[\max\left(\boldsymbol{f_n}\right)-\min\left(\boldsymbol{f_n}\right)+\min\left\{\left|\max\left(\boldsymbol{f_n}\right)-\max\left(\boldsymbol{f_n^0}\right)\right|,\left|\min\left(\boldsymbol{f_n}\right)-\max\left(\boldsymbol{f_n^0}\right)\right|\right\}\right] \quad (12)$$

Denoting the *apriori* probability of idle and busy states of the PC m as $\pi_m^0=\mathcal{P}\left[\mathcal{H}_m^0\right]$ and $\pi_m^1=\mathcal{P}\left[\mathcal{H}_m^1\right]$, respectively, the maximum achievable data rate for a normalized noise and transmission power is given by

$$R(\boldsymbol{y},\boldsymbol{X},\boldsymbol{S})=\frac{T-T_s}{T}\sum_{m\in\mathcal{M}}y_m\pi_m^0\left(1-Q_m^f\right)W_m \quad (16)$$

where $T_s=\max_n\left(T_{sw}^n(\boldsymbol{x_n})+\tau_s\boldsymbol{e_s}^T\left(\boldsymbol{x_n}\circ\boldsymbol{s_n}\right)+\tau_r\boldsymbol{e_s}^T\boldsymbol{x_n}\right)$ and W_m is bandwidth of the m^{th} PC.

We explore different scenarios and objectives to develop effective solutions with regard to various network conditions. For instance, SUs may not have enough energy resources and prefer to minimize E to save remaining battery life for future bursty traffic conditions, which will be referred to as *energy limited regime* (ELR). Alternatively, SUs may require the maximization of R in heavy traffic conditions, which will be referred to as *spectrum limited regime* (SLR). For energy and spectrum limited regimes (ESLR), on the other hand, the objective could be obtained by coupling E and R to minimize the unit energy spent per transmitted bit as follows

$$\eta\left(\boldsymbol{y},\boldsymbol{X},\boldsymbol{S}\right)=\frac{E\left(\boldsymbol{X},\boldsymbol{S}\right)}{R\left(\boldsymbol{y},\boldsymbol{X},\boldsymbol{S}\right)}\qquad[Joules/bit/s] \quad (17)$$

In the sequel, we consider η as our objective function since ELR and SLR can be considered as a special case of ESLR by treating R and E as constants in η, respectively.

B. Problem Formulation

We formulate the optimal CSS scheduling problem which will be exploited as a benchmark for the performance of the proposed heuristic methods as follows

P1: CSSS $\min_{\boldsymbol{y},\boldsymbol{X},\boldsymbol{S},\boldsymbol{\mathcal{E}}}\ \eta\left(\boldsymbol{y},\boldsymbol{X},\boldsymbol{S}\right)$

1: s.t. $Q_{th}^d\le Q_m^d\left(\tilde{\boldsymbol{P}}_{\boldsymbol{m}}^{\boldsymbol{d}}\right),\ \forall m\in\{m|\ y_m=1\}$

2: $Q_m^f\left(\tilde{\boldsymbol{P}}_{\boldsymbol{m}}^{\boldsymbol{f}}\right)\le Q_{th}^f,\ \forall m\in\{m|\ y_m=1\}$

3: $x_m^n\le y_m,\ \forall m;\forall n$

4: $\delta y_m\le\sum_n x_m^n,\ \forall m$

5: $0\le\sum_m x_m^n\le M,\ \forall m$

6: $30\le S_m^n\le\bar{S},\ \forall m;\forall n$

7: $0\le T-T_s$

8: $x_m^n,\ y_m\in\{0,1\},\ S_m^n\in\mathbb{N}^+,\ \varepsilon_m^n\in\mathbb{R},\ \forall m;\forall n$

which is an MINLP problem whose mixed-integer nature is due to the variables $\boldsymbol{y}$, $\boldsymbol{X}$ and $\boldsymbol{S}$. Lines 1 and 2 of the CSSS are the collision and spectrum utilization constraints, respectively. Line 3 simply states that if the PC m is not scheduled to be sensed then any SU cannot be assigned to sense the PC m. SUs are allowed not to sense or to sense more than one PCs in line 5 which enables SUs with low sensing and reporting attributes to save energy in sleep mode and encourages SUs with desirable attributes to discover more free PCs. Line 4, on the other hand, requires the cooperation of at least δ SUs if the PC m is scheduled to be sensed. If an SU is assigned to sense any channel, line 6 sets the lower bound of 30 on the required number of samples to invoke the central limit theorem to ensure the assumptions hold for (2) and (3) and sets the upper bound $\bar{S}=T/\tau_s$ which is the maximum number of samples possible within a timeslot duration, T. Line 7 simply limits the searching stage duration T_s to the timeslot duration T. Finally, line 8 defines the domain of the optimization variables.

Assumption 1: *As a practical approach, we assume $\boldsymbol{S}\in\mathbb{R}^{M\times N}$ to relax problem by unintegerizing the number of samples, S_m^n. Therefore, closest upper integer value can be obtained from the optimal real valued solution, which does not violate the problem constraints and has a negligible impact on the system performance since $S_m^n>>1$ and $\tau_s<<1$ in general.*

However, CSSS is still an MINLP problem due to $\boldsymbol{y}$ and $\boldsymbol{X}$ and it requires impractical time complexity even for moderate sizes of the problem. Thus, developing fast and high-performance heuristics are necessary to achieve satisfactory sub-optimal results for practical purposes. In order to develop a heuristic solution, we will focus on CSSS for a given pair of $\boldsymbol{y}$ and $\boldsymbol{X}$, CSSS($\bar{\boldsymbol{y}},\bar{\boldsymbol{X}}$) which is non-convex due to non-definite Hermitian matrix. In other words, CSSS($\bar{\boldsymbol{y}},\bar{\boldsymbol{X}}$) is a single instance of all possible combinations for real valued S.

P2: CSSS($\bar{\boldsymbol{y}},\bar{\boldsymbol{X}}$) $\min_{\boldsymbol{S},\boldsymbol{\mathcal{E}}}\ \eta(\bar{\boldsymbol{y}},\bar{\boldsymbol{X}},\boldsymbol{S})$

1: s.t. $Q_{th}^d\le Q_m^d\left(\tilde{\boldsymbol{P}}_{\boldsymbol{m}}^{\boldsymbol{d}}\right),\ \forall m\in\{m|\ y_m=1\}$

2: $Q_m^f\left(\tilde{\boldsymbol{P}}_{\boldsymbol{m}}^{\boldsymbol{f}}\right)\le Q_{th}^f,\ \forall m\in\{m|\ y_m=1\}$

3: $30\le S_m^n\le\bar{S},\ \forall m;\forall n$

4: $0\le T-T_s$

5: $S_m^n\in\mathbb{R}^+,\ \varepsilon_m^n\in\mathbb{R},\ \forall m;\forall n$

In the sequel, we convert the CSSS($\bar{\boldsymbol{y}},\bar{\boldsymbol{X}}$) into an equivalent convex problem based on the following remark and lemmas since it will be exploited to develop heuristic solutions in the next section.

Remark 1: *For a composite function, $a=b\circ c$, convex composition rules are given as [20]*

1) *a is convex if b is convex and non-increasing, and c is concave.*
2) *a is concave if b is concave and non-increasing, and c is convex.*

Lemma 1 (Decoupled Convexity)**:** *Denoting the inside expressions of (2) and (3) as g and h, respectively, and assuming $P_{m,n}^f\le0.5,\ P_{m,n}^d\ge0.5,\ \forall m,n,\ \mathcal{Q}(g)\le0.5$ ($\mathcal{Q}(h)\ge0.5$) is a decreasing convex (concave) function. Moreover,*

1) *For a feasible $S_m^n,\ \bar{S}_m^n$, g and h are both increasing*

and linear functions of ε_m^n. Thus, $P_{m,n}^f$ $\left(P_{m,n}^d\right)$ is a decreasing convex (concave) function of ε_m^n.

2) *For a feasible ε_m^n, $\bar{\varepsilon}_m^n$, g (h) is an increasing (decreasing) concave (convex) function of S_m^n. Thus, $P_{m,n}^f$ $\left(P_{m,n}^d\right)$ is a decreasing (increasing) convex (concave) function of S_m^n.*

Proof: Please see Appendix A.

Lemma 2: *Monotonicity and parameterized convexity (concavity) of $P_{m,n}^f$ ($P_{m,n}^d$) also holds for the reported false alarm and detection probabilities $\tilde{P}_{m,n}^f$ ($\tilde{P}_{m,n}^d$). **Proof:** Please see Appendix A.*

Lemma 3: *$\eta\left(\bar{\boldsymbol{y}}, \bar{\boldsymbol{X}}, \boldsymbol{S}\right)$ is a monotonically increasing function of the number of samples, S_m^n, $\forall m, n$. **Proof:** Please see Appendix A.*

Exploiting the convex composition rules in Remark 1, Lemmas 1 and 2 are first introduced to show the monotonicity and decoupled convexity of the reported local false alarm and detection probabilities. Please note that the conditions of $P_{m,n}^f \leq 0.5$ and $P_{m,n}^d \geq 0.5$ do not conflict with the practical range of interest as discussed in Section VI-A. Consequently, exploiting the decoupled convexity of the problem, Theorem 1, and the log-concavity of the Poisson-Binomial distribution (also the Binomial distribution as a special case) [9] , CSSS($\bar{\boldsymbol{y}}, \bar{\boldsymbol{X}}$) can equivalently be written as a convex problem as follows

$$
\begin{aligned}
&\textbf{P3:} \quad \min_{\boldsymbol{S}_m, \boldsymbol{\mathcal{E}_m}} \quad \eta\left(\bar{\boldsymbol{y}}, \bar{\boldsymbol{X}}, \boldsymbol{S}\right) \\
&1: \quad \text{s.t.} \quad \log\left(Q_{th}^d\right) \leq \log\left(Q_m^d\left(\tilde{\boldsymbol{P}}_{\boldsymbol{m}}^{\boldsymbol{d}}\right)\right) \\
&2: \quad \log\left(Q_m^f\left(\tilde{\boldsymbol{P}}_{\boldsymbol{m}}^{\boldsymbol{f}}\right)\right) \leq \log\left(Q_{th}^f\right) \\
&3: \quad 1 \leq \varepsilon_m^n \leq \gamma_m^n + 1, \ \forall n \\
&4: \quad 30 \leq S_m^n \leq \bar{S}, \ \forall n \\
&5: \quad 0 \leq T - T_s \\
&6: \quad S_m^n \in \mathbb{R}^+, \ \varepsilon_m^n \in \mathbb{R}, \ \forall n
\end{aligned}
$$

where $\boldsymbol{S}_m$ and $\boldsymbol{\mathcal{E}}_m$ are the m^{th} row vectors of $\boldsymbol{S}$ and $\boldsymbol{\mathcal{E}}$, respectively. Taking the logarithm of global detection and false alarm probabilities is to ensure the convexity of the objective, Line 1, and Line 2 using the log-concavity of the Poisson-Binomial distribution. Line 3 satisfies the requirement $P_{m,n}^f \leq 0.5$, $P_{m,n}^d \geq 0.5$, $\forall m, n$. P3 can be solved using primal decomposition methods, that is, P3 is separated into two levels of optimization. At the lower level, we have a convex problem of ε by fixing S. At the higher level, on the other hand, we have a master convex problem of S by fixing ε. Since $\eta\left(\bar{\boldsymbol{y}}, \bar{\boldsymbol{X}}, \boldsymbol{S}\right)$ is a differentiable objective function, then the master problem can be solved with a gradient method [21].

Based on Theorem 1, optimal values of sensing duration and detection thresholds under the homogeneous mode can be calculated using the closed form expressions as in Theorem 2.

Theorem 1: *For a feasible detection threshold $\bar{\varepsilon}_m^n$, the optimal $\eta\left(\bar{\boldsymbol{y}}, \bar{\boldsymbol{X}}, \boldsymbol{S}\right)$ that satisfies the constraint $Q_m^d \geq Q_{th}^d$ is attained at S_m^n which satisfies $Q_m^d = Q_{th}^d$. For a given $\bar{S}_m^n$, on the other hand, the optimal $\eta\left(\bar{\boldsymbol{y}}, \bar{\boldsymbol{X}}, \boldsymbol{S}\right)$ that satisfies the constraint $Q_m^f \leq Q_{th}^f$ is attained at ε^n which satisfies $Q_m^f = Q_{th}^f$. **Proof:** Please see Appendix B.*

Theorem 2: *Contingent upon Theorem 1, required local false alarm and detection probabilities for a given SU assignment matrix $\bar{\boldsymbol{X}}$ is expressed as*

$$P_{m,n}^{f^\star} = \frac{\tilde{P}_m^{f^\star} - p_m^n}{1 - 2p_m^n} \tag{18}$$

$$P_{m,n}^{d^\star} = \frac{\tilde{P}_m^{d^\star} - p_m^n}{1 - 2p_m^n} \tag{19}$$

where $\tilde{P}_m^{f^\star} = \{\tilde{P}_m^f \mid Q_m^f = Q_{th}^f, C\}$ and $\tilde{P}_m^{d^\star} = \{\tilde{P}_m^d \mid Q_m^d = Q_{th}^d, C\}$ are target false alarm and detection probabilities of each SU for a given cluster size, C. Accordingly, optimal S_m^n and ε_m^n under the homogeneous mode are given by

$$S_{m,n}^\star = \left[\frac{\mathcal{Q}^{-1}\left(P_{m,n}^{d^\star}\right)\sqrt{2\gamma_m^n + 1} - \mathcal{Q}^{-1}\left(P_{m,n}^{f^\star}\right)}{\gamma_m^n}\right]^2 \tag{20}$$

$$\varepsilon_{m,n}^\star = 1 + \frac{\mathcal{Q}^{-1}\left(P_{m,n}^{f^\star}\right)}{\sqrt{S_{m,n}^\star}} \tag{21}$$

Proof: *Please see Appendix B.*

V. Energy & Spectrum Efficient Heuristics

A. Prioritized Ordering Heuristic (POH)

We first begin with a channel ordering heuristic which prioritizes channels according to the regime type as shown in Algorithm 1. POH provides us with an optimistic channel prioritization such that how solely scheduling a single PC can perform if we greedily assign the best δ SUs to it. For every PC, Algorithm 1 first orders SUs with respect to their SNR values on PC m and record this sorting in the list $\bar{\boldsymbol{\gamma}}_{\boldsymbol{m}}$. Thereafter, it forms $\bar{\boldsymbol{y}}$ with zero entries except at the m^{th} position and $\bar{\boldsymbol{X}}$ with zero entries except the first δ SUs of $\bar{\boldsymbol{\gamma}}_{\boldsymbol{m}}$. We denote the performance metrics of PC m as $\langle \eta_m, E_m, R_m \rangle$ where $\eta_m = E_m / R_m$, E_m, and R_m respectively represent the induced energy efficiency, total energy consumption and the total achievable data rate from scheduling the PC m to be sensed. $\langle \eta_m, E_m, R_m \rangle$ is then calculated under the heterogeneity or homogeneity mode using P3 and (20), respectively. Finally, PCs are sorted with respect to R_m, E_m and η_m under the SLR, ELR and ESLR, respectively.

Algorithm 1 POH

Input: $\boldsymbol{P}$, $\boldsymbol{\Gamma}$, δ
Output: Prioritized channel vectors and descending sorted $\boldsymbol{\Gamma}$

```
for m = 1 to M do
    γ̄_m ← Sort SUs in descending order wrt γ_m^n
    ȳ ← Schedule only channel m to be sensed
    X̄ ← Assign the best δ SUs to channel m from γ̄_m.
    S ← Compute ⟨η_i, E_i, R_i⟩ by P3 (Theorem 2) in heterogeneous (homogeneous) mode.
end for
Γ̄ ← Form ordered Γ from γ̄_m, ∀m.
c_R ← Sort channels in descending order wrt R_m.
c_E ← Sort channels in ascending order wrt E_m.
c_η ← Sort channels in ascending order wrt η_m.
return c_η, c_E, c_R, Γ̄.
```

One of the key features of the proposed heuristic is the assignment of exactly δ SUs which is the minimum requirement for the cluster size. The underlying reason is that the total number of samples to meet the global detection and false alarm probabilities increases as the cluster size increases even if the required individual number of samples decreases because of the increase (decrease) in $\tilde{P}_m^{f^\star}$ ($\tilde{P}_m^{d^\star}$) by adding one more SU. Although it is not trivial to show this behavior analytically due to the lack of closed form $\mathcal{Q}$-function expression, variations in total number of samples, $\tilde{P}_m^{f^\star}$, and $\tilde{P}_m^{d^\star}$ are numerically evaluated in Section VI. Likewise, reporting and switching energy consumption also increase with the cluster size since the number of reports and possible channel switching may occur with additional SUs. While the outer loop takes $\mathcal{O}[M]$ steps, sorting operations in Line 2 and Lines 12-14 are $\mathcal{O}[N \log N]$ and $\mathcal{O}[M \log M]$, respectively. Denoting the number of iterations for **P3** by I, the computation of performance metrics between lines 5-9 takes $\mathcal{O}[M\delta]$ ($\mathcal{O}[MI]$) steps in the homogeneous (heterogeneous) mode. Therefore, the overall complexity of POH in homogeneous (heterogeneous) mode is $\mathcal{O}[M(N \log N + \delta) + M \log M]$ ($\mathcal{O}[M(N \log N + I) + M \log M]$), and since we assume that $N \geq M$, the complexity is $\mathcal{O}[M(N \log N + \delta)]$ ($\mathcal{O}[M(N \log N + I)]$).

B. Scheduling and Assignment Heuristic (SAH)

Exploiting the POH outputs and following the initialization process, SAH schedules the first i channels from $\boldsymbol{c_R}$ / $\boldsymbol{c_\eta}$ / $\boldsymbol{c_E}$ under the SLR / ELR / ESLR, and greedily assigns the best δ SUs from $\bar{\mathbf{\Gamma}}$. Afterwards, based on the heterogeneity or homogeneity mode preference, $\langle \eta_m,\ E_m,\ R_m \rangle$ is calculated using P3 and (20), respectively. Based on the difference in the objective function between successive iterations, Δ, the algorithm determines if there is a decrease (increase) in η and E (R) by scheduling i^{th} PC from the prioritized channel vector and updates the best solution space. The termination condition of the while loop is satisfied if either there is no performance enhancement by the addition of the i^{th} PC, or there is no PC left to schedule. In the SLR, SAH will run at most M iterations since it seeks the largest possible data rate without being concerned about the opportunity cost. Since scheduling more channels will increase the opportunity cost, the best case is not scheduling any PC so that the optimal total energy consumption is zero under the ELR. However, SAH mitigates this best but impractical case by scheduling only the most energy efficient PC. Thus, while the time complexity under the ELR is constant, that under other regimes is $\mathcal{O}[M\delta]$ ($\mathcal{O}[MI]$) in homogeneous (heterogeneous) modes.

Algorithm 2 SAH

Input: $\boldsymbol{P}$, $\bar{\mathbf{\Gamma}}$, δ, $\boldsymbol{c_\eta}/\boldsymbol{c_E}/\boldsymbol{c_R}$
Output: The best solution with the corresponding $\bar{\boldsymbol{y}}$ and $\bar{\boldsymbol{X}}$.
1: $\Delta \leftarrow 0$
2: $i \leftarrow 1$
3: $\eta_0 \leftarrow \infty$ / $E_0 \leftarrow \infty$ / $R_0 \leftarrow -\infty$
4: $\mathcal{S}^\star \leftarrow \langle \eta_0,\ E_0,\ R_0 \rangle$
5: **while** $\Delta \leq 0$ && $i \leq M$ **do**
6: $\quad \bar{\boldsymbol{y}} \leftarrow$ Schedule the best i channels in $\boldsymbol{c_\eta}$
7: $\quad \bar{\boldsymbol{X}} \leftarrow$ Assign the best δ SUs to channels from $\bar{\mathbf{\Gamma}}$.
8: $\quad \mathcal{S} \leftarrow$ Compute $\langle \eta_i,\ E_i,\ R_i \rangle$ by P3 (Theorem 2) in heterogeneous (homogeneous) mode.
9: $\quad \Delta \leftarrow \begin{cases} \eta_i - \eta_{i-1}, & \text{under ESLR} \\ E_i - E_{i-1}, & \text{under ELR} \\ R_{i-1} - R_i,, & \text{under SLR} \end{cases}$
10: $\quad$ **if** $\Delta \leq 0$ **then**
11: $\quad\quad \mathcal{S}^\star \leftarrow \langle \eta_i,\ E_i,\ R_i \rangle$
12: $\quad$ **end if**
13: $\quad i \leftarrow i + 1$
14: **end while**
15: **return** $\mathcal{S}^\star$, $\bar{\boldsymbol{y}}$, $\bar{\boldsymbol{X}}$

Par.	Value	Par.	Value	Par.	Value
P_s	1 W [7], [13], [22]	τ_s	1 μs	Q_{th}^f	0.01
P_x	1 W [7] , [13], [11], [22]	τ_r	1 ms [7], [13]	Q_{th}^d	0.99
P_{sw}	1 W [7] , [13], [11]	β	0.1 ms/MHz [7] , [13], [11]	T	2 s
θ_m^n	2,	$\sigma_{\varphi_m^n}$	5	d_0	10 m

Table I: Default parameters used for obtaining results

VI. Results and Analysis

All simulation results were obtained and plotted using Matlab. Throughout the simulation, the values in Table I are employed, unless it is explicitly stated otherwise. These values are adopted from the references shown in the table.

A. Relationship among Cluster Size, Energy, $P_f^\star$, and $P_d^\star$

In Fig. 3, total number of samples of SUs versus the cluster size ranging from 1 to 100 is depicted along with the corresponding $\tilde{P}_f^\star$ and $\tilde{P}_d^\star$ values which ensure Q_{th}^f and Q_{th}^d, respectively. Curves with diamond, square and circle shaped markers show homogeneous clusters which consist of SUs with identical SNRs of -5, -10 and -15 dB, respectively. The curve with the star shaped markers, on the other hand, considers a heterogeneous cluster which consists of non-identical SUs such that the cluster size C on the x-axes composed of the best C SUs among 100 SUs with SNRs range from -20 and 0 dB. In both cases, the total number of samples, hence the total sensing energy, increases with the cluster size. This increase is much more significant in the heterogeneous case that asymptotically approaches its mean value (-10 dB) and -10 dB homogeneous case with diamond shapes. Since the total sensing energy cost increases with the cluster size under both modes, the optimal energy cost is obtained by assigning exactly δ SUs for each scheduled PC. As can be seen from below subplot, enforcing SUs to have $P_{m,n}^f \leq 0.5$ and $P_{m,n}^d \geq 0.5$ does not contradict with practicality since $P_f^\star$ and $P_d^\star$ are still far away from those limits even for an

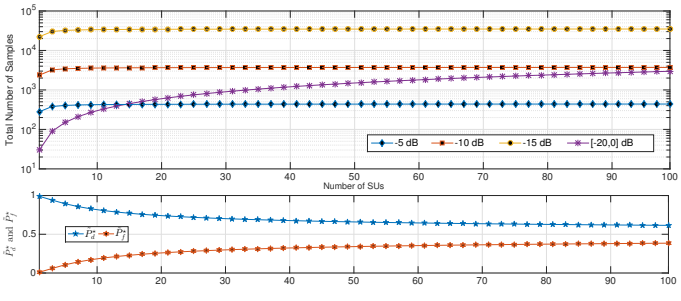

Fig. 3: Total S_m^n, $\tilde{P}_d^\star$, and $\tilde{P}_f^\star$ vs. cluster size.

impractically large cluster sizes.

B. Comparison Between Optimal and Heuristic Solutions

Fig. 4 shows the comparison between the optimal exhaustive benchmark and heuristic solutions for an average of 30 CRN scenarios each of which comprises of 4 PCs and 8 SUs with SNRs which follows the following combined path loss and shadowing model [17]

$$P^r_{m,n} = P^t_m K_m \left[\frac{d_0}{d^n_m}\right]^{\theta_m} \varphi^n_m \tag{22}$$

where $\mathbb{P}^t_m$ and $\mathbb{P}^r_{m,n}$ represent the transmitted signal power by PU m and the received signal power by SU n on the PC m, respectively; K_m is a unitless constant that depends on the primary signal wavelength and the reference distance d_0; θ_m is the path-loss exponent that represents the rate at which the path loss increases with the distance between the SU n and the PU m, d^n_m; and φ^n_m is the log normal shadowing component which follows normal distribution in dB scale, $\mathcal{N}\left(0, \sigma^2_{\varphi^n_m}\right)$, respectively.

The solid blue and red curves draw the optimal homogeneous (Binomial) and heterogeneous (Poisson-Binomial) modes, respectively. Similarly, the dashed curves with diamond and square shapes show the heuristic performance, which minimizes η using SAH with the given prioritized channel order $\boldsymbol{c}_\eta$ returned from POH, for homogeneous and heterogeneous modes, respectively. While the subplot (a) depicts the objective itself, subplot (b) and (c) demonstrate the corresponding opportunity cost (E) and the remaining time ($T - T_s$) for the secondary data transmission, respectively. It is clear from the figure that the proposed heuristic approach performance is very close to that of the benchmark in both modes. Taking heterogeneity into account gives a superior performance over using homogeneity assumption for $\delta \geq 3$. This is because the homogeneous assumption requires SUs with relatively low SNRs to obtain exact local detection performance of SUs with relatively high SNRs. In other words, if cluster members have a broad range of SNRs, heterogeneous mode shows superior performance than the homogeneous mode. On the contrary, if SUs have identical SNRs (i.e. cluster is homogeneous in reality and range of SNRs is zero) considering heterogeneity will not make any difference.

Furthermore, the reasoning behind the assignment of exactly δ SU is now more obvious due to the increasing trend of η with regard to δ. This is because of increasing sensing energy (as shown in Fig. 3), reporting+switching energy since since involving more SUs in sensing requires more reports and possibly more channel switches. Another significance of considering heterogeneity is revealed in subplot (c) where available time left for the secondary transmission is dramatically reduced in the homogeneous case as the slowest SU is enforced to have identical performance with others, which directly reduces the achievable throughput. Subplots (d), (e) and (f) detail the cost factors of the opportunity cost. As can be seen, reporting and switching energy consumption is very close to the sensing energy for the heterogeneous mode for all δ values. However, sensing energy becomes more significant in the homogeneous mode for higher δ values since we enforce low SNR SUs to sense with identical detection performance. Moreover, reporting and switching energy consumption increase with δ because the number of channel switches and reports increase with the number of assigned SUs.

Likewise, Fig. 5 shows the comparison between the optimal exhaustive benchmark and heuristic solutions for an average of 30 CRN scenarios each of which consists of 8 PCs and 4 SUs with SNRs randomly selected between 0 and -10 dB. Even though we will not go over the underlying reasons of the curves, we will point out the following: The proposed heuristic still gives very close performance to the optimal approach and follows the same trend. Since the average SNR values is $-5dB$ and the SNR range is tight, the difference between the heterogeneous and homogeneous modes is not as significant as in Fig. 4. However, we note that opportunity cost factors shows very close values due to the relatively high SNR values in comparison to these in Fig. 4.

C. Numerical Results for SAH

Fig. 6 demonstrates the behavior of η, E and R under different regimes with respect to different numbers of SUs and PUs, and SNR distributions in subplots (a), (b) and (c), respectively. While the solid green, blue and red lines correspond to the homogeneous mode under the ESLR, ELR, and ESR, respectively, the dashed lines with the corresponding colors are used for heterogeneous mode. We first note that the best η performance is always obtained under the ESLR regime using $\boldsymbol{c_\eta}$. Similarly, the best E and R performance is always observed under the ELR and ESR regimes using $\boldsymbol{c_E}$ and $\boldsymbol{c_R}$, respectively. On the other hand, the worst case of E (R) occurs under the SLR (ELR) since it does not care about energy (spectrum) during the channel ordering and SU assignment phases. However, η gives a middling E and R performance all the time since it couples both of them.

Fig. 6-(a) shows the changes with respect to the number of SUs ranging from 8 to 160 for $M = 20$ and random SNRs between -30 dB and 0 dB. As the number of SUs increases, R under the SLR increases in every $\delta = 8$ steps since having a new set of δ SUs allows SAH to schedule one more PC. E under the SLR first decreases until $N = 20$ and then it starts to increase. This is primarily because small increments in the number of SUs have more significant SU diversity if the number of channels is relatively high in comparison to number of channels. However, heterogeneity modes have a slight impact for $N \geq 20$ because network has more SU diversity and SNR range of the best δ SUs is tight due to the ordering. The increase of E under the SLR after $N = 20$ is directly related to the greedy demand for scheduling more channels. Therefore, η under the SLR is a result of the behavior of E and R and it gives the worst performance among the three schemes. E under the ELR is the best case and has a decreasing nature with respect to N, which is because of increasing SU assignment diversity and high chance of finding high SNR SUs to sense the most energy efficient channel. On the contrary, R under the ELR follows a mean value of 0.5 $Mbps$ since it only schedules the most energy efficient channel

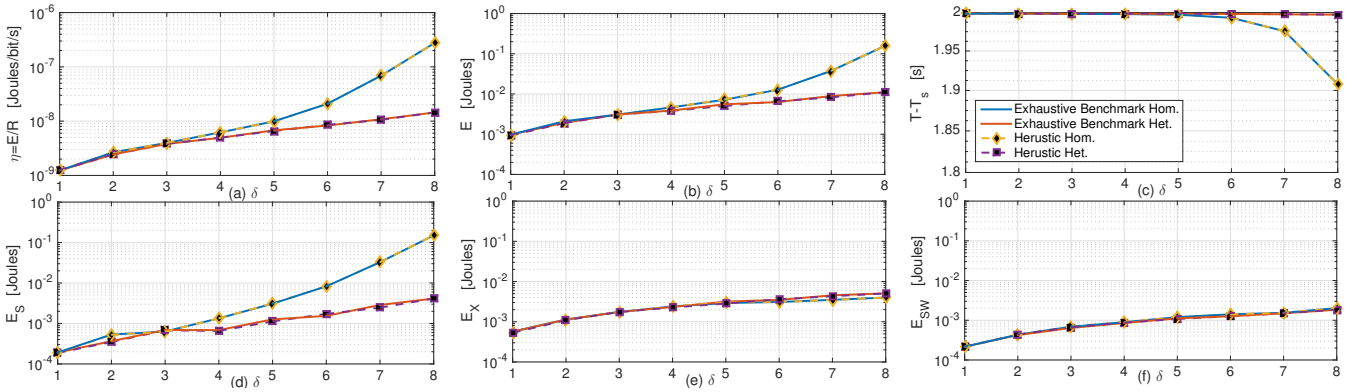

Fig. 4: Comparison between the optimal and heuristic solutions for an average of 30 CRN scenarios with 4 PCs and 8 SUs with SNRs randomly selected between 0 and -30 dB for different values of δ: (a) η, (b) E, (c) $T - T_s$, (d) E_S, (e) E_X, and (f) E_{SW}.

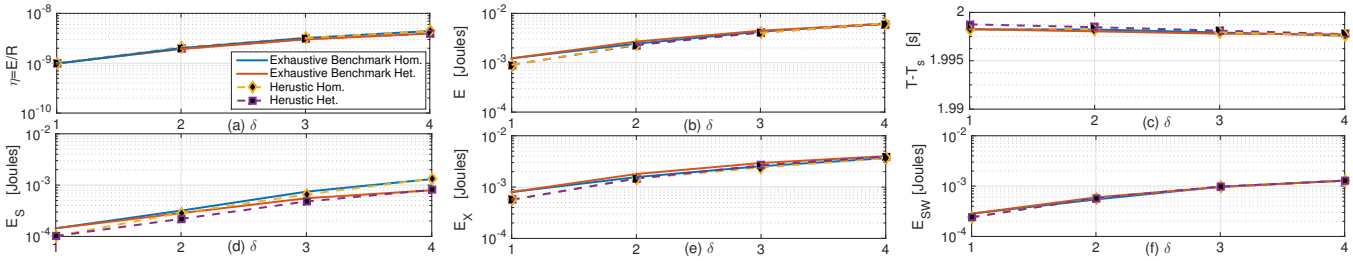

Fig. 5: Comparison of optimal and heuristic solutions for an average of 30 CRN scenarios with 8 PCs and 4 SUs with SNRs randomly selected between 0 and -10 dB for different values of δ: (a) η, (b) E, (c) $T - T_s$, (d) E_S, (e) E_X, and (f) E_{SW}.

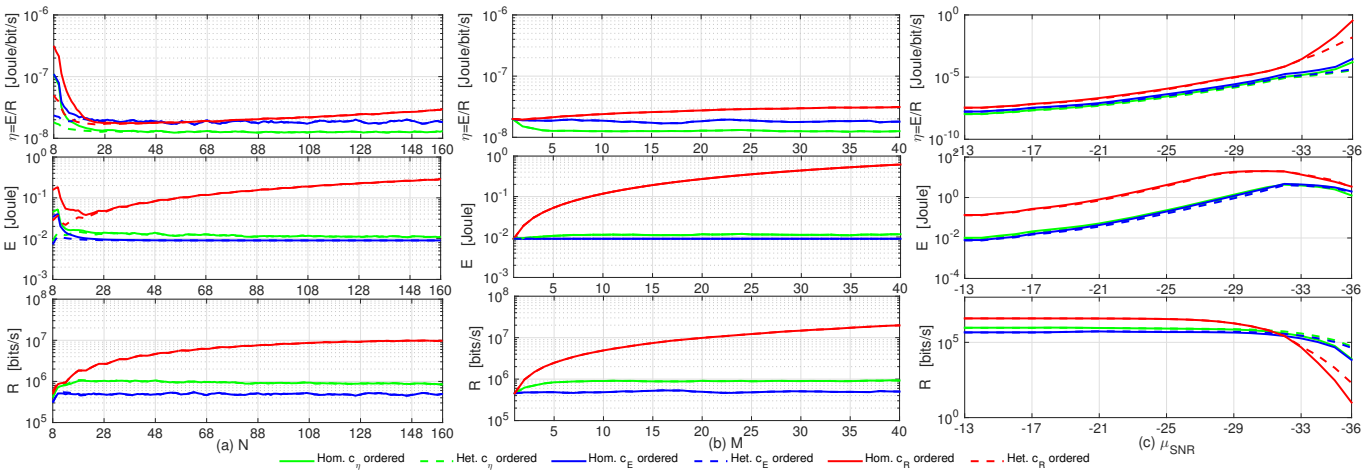

Fig. 6: SAH results over 100 CRN scenarios with $M = 20$, $N = 100$, SNRs range from -30 to 0 dB and $\delta = 8$. Behaviors of η, E and R under different regimes with respect to (a) number of SUs, (b) number of PUs and (c) mean SNRs.

and PCs have an average apriori probability of 0.5, which is the worst case among others. As stated earlier, E and R under the ESLR regime provide a middling performance since it is not greedy either for E or R. As expected, it gives the best η performance since ordering and SU assignment is made based on η.

Fig. 6-(b) shows the performance for the number of PCs ranging from 1 to 40 for $N = 100$ and random SNRs between -30 dB and 0 dB. Under the SLR, R monotonically increases with the number of PCs which is because of the increasing chance of finding PCs with higher apriori probabilities. Accordingly, E under the SLR increases with the R since more SUs are involved to sense more PCs, so does η. However, R, E, thus η remain almost constant under the ELR since the number of SUs is fixed and ELR only selects the most energy efficient channel which yields an average of 0.5 $Mbps$ data rate. Although E and R slightly increases with the number of PCs under the ESLR, η slightly decreases since R has a higher increasing peace than the E.

For $M = 20$ for $N = 100$, Fig. 6-(c) shows the changes with respect to SNR scenarios where SNR distribution follows a normal distribution with variance 10 dB and mean values on

x-axes. Although R does not experience a significant change until $28-30$ dB, E significantly increases with mean SNR of SUs. Despite of the decrease in the mean SNR and thus the increase in total number of samples, SAH is able to find some PCs with low opportunity cost. After $28-30$ dB, however, most of the PCs become infeasible to schedule due to the poor sensing quality of the entire SUs. Accordingly, SAH tends to schedule very few number of PCs due to SUs' infeasibly high sensing cost, that is why R and E start to decrease. Behavior of η is simply a natural outcome of the underlying reasons we gave for E and R.

VII. Conclusions

In this paper, we considered a multi-channel CSS scheduling framework to minimize the induced sensing, reporting and channel switching energy per obtained opportunity subject to the global detection and spectrum utilization constraints. Different from previous works, we factor the reporting error in and provide a general scheme which can be applied to any voting rule. After formulating an optimal MINLP problem, we develop an equivalent convex framework for specific instances of combinatorial solution space. In this way, we were able to develop very efficient, yet fast heuristics for different regimes regarding the energy limitations and data rate demands the performance of which is compared to the exhaustive benchmark solution. We have also illustrated the impact of heterogeneity and homogeneity assumption under different network scenarios. Results show that the taking the heterogeneity into account yield a low total sensing cost and high time left for SU transmission since the proposed heterogeneous mode also decreases the sensing duration of the slowest SU.

Appendix A
Decoupled Convexity Analysis of CSSS$\left(\bar{\boldsymbol{y}}, \bar{\boldsymbol{X}}\right)$

Proof of Lemma 1: Throughout the appendices, we omit cluster and SU indices, m and n, for the sake of notational convenience without loss of generality. $\mathcal{Q}(\cdot)$ is a non-increasing convex (concave) function in the case of $\mathcal{Q}(\cdot) \leq 0.5$ ($\mathcal{Q}(\cdot) \geq 0.5$), respectively. This can be easily satisfied by constraining the detection threshold as

$$1 \leq \varepsilon \leq \gamma + 1 \tag{23}$$

which follows from the fact that S is non-negative. To meet the composition requirements of $P^f = \mathcal{Q}(g)$ ($P^d = \mathcal{Q}(h)$) as in Remark 1, g (h) is still required to be jointly concave (convex) in (S, ε). Unfortunately, this is not the case since the Hessian matrix of g in (24) and that of h in (25) are neither positive nor negative semi-definite as follows

$$\bigtriangledown^2 g(S,\varepsilon) = \begin{bmatrix} \frac{(1-\varepsilon)}{4S^{3/2}} & \frac{1}{2\sqrt{S}} \\ \frac{1}{2\sqrt{S}} & 0 \end{bmatrix} \tag{24}$$

$$\bigtriangledown^2 h(S,\varepsilon,\gamma) = \begin{bmatrix} \frac{(\gamma+1-\varepsilon)}{4S^{3/2}\sqrt{2\gamma+1}} & \frac{1}{2\sqrt{S(2\gamma+1)}} \\ \frac{1}{2\sqrt{S(2\gamma+1)}} & 0 \end{bmatrix} \tag{25}$$

Therefore, local probabilities $P^f(g)$ and $P^d(h)$ are neither convex nor a concave function of (S, ε). As a consequence, this result directly affects the convexity (concavity) of Q_m^f (Q_m^d), and **CSSS**($\bar{\boldsymbol{y}}$,$\bar{\boldsymbol{X}}$). For a fixed (parameterized) feasible number of samples $\bar{S}$, however, g and h are both linear functions of ε due to the zero terms in (24)-(25) and decreasing functions due to (23). Based on Remark 1, $P^f(g)$ ($P^d(h)$) is a decreasing convex (concave) function of ε for a given $\bar{S}$. On the other hand, g (h) is an increasing concave (decreasing convex) function of S for a parameterized feasible detection threshold $\bar{\varepsilon}$ since $\frac{(1-\varepsilon)}{4S^{3/2}} \leq 0$ $\left(\frac{(\gamma+1-\varepsilon)}{4S^{3/2}\sqrt{2\gamma+1}} \geq 0\right)$ if (23) is satisfied. According to Remark 1, $P^f(g)$ ($P^d(h)$) is an decreasing convex (increasing concave) function of S for a given $\bar{\varepsilon}$ ■

Proof of Lemma 2: The parameterized convexity in Lemma 2 can be further applied to the received local probabilities $\tilde{P}^f$ and $\tilde{P}^d$ since (4) and (5) are nothing but the non-negative weighted summation of P^f (P^d). ■

Proof of Lemma 3: We first note that $E\left(\bar{\boldsymbol{X}}, \boldsymbol{S}\right)$, is a linear function of number of samples since T_{sns} is the summation of number of samples while T_{sw} and T_r are both constant with respect to S. As a consequence, $E\left(\bar{\boldsymbol{X}}, \boldsymbol{S}\right)$ increases as the S increases. $R\left(\bar{\boldsymbol{y}}, \bar{\boldsymbol{X}}, \boldsymbol{S}\right)$ is a concave decreasing function of S as per the piece-wise maximization of convex functions is convex [20], T is a constant, and T_s is negated in $\frac{T-T_s}{T}$. [1] For an increase in S, $R\left(\bar{\boldsymbol{y}}, \bar{\boldsymbol{X}}, \boldsymbol{S}\right)$ either decreases, if the SU n is the slowest SU which determines the T_s, or stay unchanged. Therefore, $\eta\left(\bar{\boldsymbol{y}}, \bar{\boldsymbol{X}}, \boldsymbol{S}\right)$ monotonically increases as S increases. ■

Appendix B
Proof of Theorem 1 and Theorem 2

Proof of Theorem 1: As stated in Lemma 2, $\tilde{P}^f$ ($\tilde{P}^d$) is a decreasing (increasing) convex (concave) function of S for a given $\bar{\varepsilon}$. Thus, for a feasible detection threshold $\bar{\varepsilon}$ and increasing S, while P^f and Q^f decrease, P^d, Q^d, and η increase. Since increasing the S causes increase in $\eta\left(\bar{\boldsymbol{y}}, \bar{\boldsymbol{X}}, \boldsymbol{S}\right)$ according to Lemma 3, optimal $\eta\left(\bar{\boldsymbol{y}}, \bar{\boldsymbol{X}}, \boldsymbol{S}\right)$ attained once S_m^n satisfies $Q^d \geq Q_{th}^d$, i.e., $Q^d = Q_{th}^d$. Similarly, $\tilde{P}^f$ ($\tilde{P}^d$) is a decreasing convex (concave) function of ε for a given $\bar{S}$. For a given $\bar{S}$ and decreasing ε, on the other hand, P^d, Q^d, P^f, and Q^f increase, which is upper-bounded by $Q^f \leq Q_{th}^f$. Thus, the optimal value of ε_m^n is attained at $Q^f = Q_{th}^f$. ■

Proof of Theorem 2: Under the homogeneous mode, SUs are enforced to provide identical local false alarm and detection probability reports, i.e. $\tilde{P}_{m,n}^f = \tilde{P}_m^f$ and $\tilde{P}_{m,n}^d = \tilde{P}_m^d$, $\forall n \in \mathcal{C}_m$. In such a case, there is no need to solve P3 numerically since distinguishing sensing durations and detection thresholds of each SU is unnecessary. Therefore, Q_m^f (Q_m^d) directly becomes a function of $\tilde{P}_m^f$ ($\tilde{P}_m^d$) whose optimal value, $\tilde{P}_m^{f^\star} = \{\tilde{P}_m^f \mid Q_m^f = Q_{th}^f\}$ $\left(\tilde{P}_m^{d^\star} = \{\tilde{P}_m^d \mid Q_m^d = Q_{th}^d\}\right)$ could simply be computed using the bisection method. As shown in Fig. 3, there is also a close relationship between the cluster size and $\tilde{P}_m^{f^\star}$ ($\tilde{P}_m^{d^\star}$) such that as the cluster size

[1] We assume that the Q_m^f is constant since it is Q_{th}^f at the optimal point as explained in Theorem 1.

increases $\tilde{P}_m^{f^\star}$ ($\tilde{P}_m^{d^\star}$) increases (decreases). Rewriting (4) and (5) as

$$\tilde{P}_m^{f^\star} = p_m^n \left(1 - P_{m,n}^{f^\star}\right) + \left(1 - p_m^n\right) P_{m,n}^{f^\star} \tag{26}$$

$$\tilde{P}_m^{d^\star} = p_m^n \left(1 - P_{m,n}^{d^\star}\right) + \left(1 - p_m^n\right) P_{m,n}^{d^\star}, \tag{27}$$

assuming $p_m^n < 0.5$, $\forall m, n$, and solving (26) and (27) for $P_{m,n}^{f^\star}$ and $P_{m,n}^{d^\star}$, required local false alarm and detection probabilities can be found as in (18) and (19), respectively. Indeed, $p_m^n \simeq 0.5$ has already shown to be the imperfect reporting error wall beyond which the reliable CSS is not possible no matter how much energy is spent on sensing [9]. Finally, substituting (18) and (19) into the right hand side of (2) and (3), and then solving (2) and (3) for S_m^n and ε_m^n, the optimal number of samples and detection thresholds are derived as in (20) and (21), respectively. ■

REFERENCES

[1] S. Pollin, R. Mangharam, B. Bougard, L. Van der Perre, I. Moerman, R. Rajkumar, and F. Catthoor, "Meera: Cross-layer methodology for energy efficient resource allocation in wireless networks," *IEEE Transactions on Wireless Communications*, vol. 7, no. 1, pp. 98–109, 2008.

[2] G. Gur and F. Alagoz, "Green wireless communications via cognitive dimension: an overview," *IEEE Network*, vol. 25, no. 2, pp. 50–56, 2011.

[3] M. Webb *et al.*, "Smart 2020: Enabling the low carbon economy in the information age," *The Climate Group. London*, vol. 1, no. 1, pp. 1–1, 2008.

[4] R. Deng, J. Chen, C. Yuen, P. Cheng, and Y. Sun, "Energy-efficient cooperative spectrum sensing by optimal scheduling in sensor-aided cognitive radio networks," *IEEE Transactions on Vehicular Technology*, vol. 61, no. 2, pp. 716–725, 2012.

[5] T. Zhang and D. H. Tsang, "Optimal cooperative sensing scheduling for energy-efficient cognitive radio networks," in *proc. IEEE INFOCOM*. IEEE, 2011, pp. 2723–2731.

[6] X. Sun and D. H. Tsang, "Energy-efficient cooperative sensing scheduling for multi-band cognitive radio networks," *IEEE Transactions on Wireless Communications*, vol. 12, no. 10, pp. 4943–4955, 2013.

[7] S. Eryigit, S. Bayhan, and T. Tugcu, "Energy-efficient multichannel cooperative sensing scheduling with heterogeneous channel conditions for cognitive radio networks," *IEEE Transactions on Vehicular Technology*, vol. 62, no. 6, pp. 2690–2699, 2013.

[8] S. Chaudhari, J. Lunden, V. Koivunen, and H. V. Poor, "Cooperative sensing with imperfect reporting channels: Hard decisions or soft decisions?" *IEEE Transactions on Signal Processing*, vol. 60, no. 1, pp. 18–28, 2012.

[9] A. Celik and A. E. Kamal, "Multi-objective clustering optimization for multi-channel cooperative spectrum sensing in heterogeneous green crns," *IEEE Transactions on Cognitive Communications and Networking*, 2016.

[10] T. Zhang and D. H. Tsang, "Cooperative sensing scheduling for energy-efficient cognitive radio networks," *IEEE Transactions on Vehicular Technology*, vol. 64, no. 6, pp. 2648 – 2662, 2015.

[11] S. Bayhan and F. Alagoz, "Scheduling in centralized cognitive radio networks for energy efficiency," *IEEE Transactions on Vehicular Technology*, vol. 62, no. 2, pp. 582–595, 2013.

[12] D. Gozupek, S. Buhari, and F. Alagoz, "A spectrum switching delay-aware scheduling algorithm for centralized cognitive radio networks," *IEEE Transactions on Mobile Computing*, vol. 12, no. 7, pp. 1270–1280, 2013.

[13] S. Eryigit, S. Bayhan, and T. Tugcu, "Channel switching cost aware and energy-efficient cooperative sensing scheduling for cognitive radio networks," in *proc. IEEE ICC*. IEEE, 2013, pp. 2633–2638.

[14] A. Celik and A. E. Kamal, "More spectrum for less energy: Green cooperative sensing scheduling in crns," in *proc. IEEE ICC*, 2015, pp. 62–67.

[15] T. Yucek and H. Arslan, "A survey of spectrum sensing algorithms for cognitive radio applications," *IEEE Communications Surveys & Tutorials*, vol. 11, no. 1, pp. 116–130, 2009.

[16] E. C. Y. Peh, Y.-C. Liang, Y. L. Guan, and Y. Zeng, "Optimization of cooperative sensing in cognitive radio networks: a sensing-throughput tradeoff view," *IEEE Transactions on Vehicular Technology*, vol. 58, no. 9, pp. 5294–5299, 2009.

[17] A. Goldsmith, *Wireless communications*. Cambridge university press, 2005.

[18] Y. H. Wang, "On the number of successes in independent trials," *Statistica Sinica*, pp. 295–312, 1993.

[19] M. Fernandez and S. Williams, "Closed-form expression for the poisson-binomial probability density function," *IEEE Transactions on Aerospace and Electronic Systems*, vol. 46, no. 2, pp. 803–817, 2010.

[20] S. Boyd and L. Vandenberghe, *Convex optimization*. Cambridge university press, 2004.

[21] D. P. Palomar and M. Chiang, "A tutorial on decomposition methods for network utility maximization," *IEEE Journal on Selected Areas in Communications*, vol. 24, no. 8, pp. 1439–1451, 2006.

[22] C. Jiang *et al.*, "Energy-efficient non-cooperative cognitive radio networks: Micro, meso, and macro views," *IEEE Communications Magazine*, vol. 52, no. 7, pp. 14–20, 2014.